UDC 543.554.6

AMPEROMETRIC DETERMINATION OF PERRHENATE ANION USING A MICROSCOPIC INTERFACES BETWEEN TWO IMMISCIBLE ELECTROLYTE SOLUTIONS

L.Yu. Martynov[1,@], E.V. Lopatukhin[1], A.A. Astafyev[2], A.M. Shakhov[2], V.A. Nadtochenko[2], N.K. Zaitsev[1]

[1]MIREA – Russian Technological University (M.V. Lomonosov Institute of Fine Chemical Technologies), Moscow 119571, Russia
[2]Semenov Institute of Chemical Physics of Russian Academy of Sciences, Moscow 119991, Russia
[@]Corresponding author e-mail: l.y.martynov@gmail.com

Voltammetric responses associated with the simple reaction of perrhenate anions transfer across polarized micro-interfaces between two immiscible electrolyte solutions (micro-ITIES) was investigated, and their sensing applications were demonstrated. The micro-ITIES array was formed at polyethylene terephthalate membranes containing a 196 microhole array of radius 10.0±0.1 μm using a femtosecond laser. The characteristics of perrhenate ions transfer at the water/2-nitrophenyloctyl ether interface were first investigated using cyclic voltammetry (CV). CV was used in the estimation of some of the perrhenate anions thermodynamic parameters, such as the formal transfer potential and the Gibbs transfer energy. The technique of alternating current stripping voltammetry (ACSV) was also utilized to improve the sensitivity of the perrhenate anion detection. Under optimized pre-concentration and detection conditions, a limit of detection of 0.3 μM with a wide linear dynamic range extending from 1.0 to 100 μM was achieved. The effect of various potential interfering anions on the perrhenate sensor was also investigated and an excellent selectivity over SCN^-, I^-, NO_3^-, NO_2^-, CO_3^{2-}, SO_4^{2-}, MoO_4^{2-}, WO_4^{2-} and CH_3COO^- ions was also achieved. This enabled quantitative measurements of rhenium in some mineral raw samples and the data was also validated by comparing with inductively coupled plasma atomic emission spectroscopy.

Keywords: *perrhenate ion, water/2-nitrophenyloctyl ether interface, micro-ITIES, ion transfer reaction, femtosecond laser, stripping voltammetry.*

DOI: 10.32362/2410-6593-2018-13-4-5-16

АМПЕРОМЕТРИЧЕСКОЕ ОПРЕДЕЛЕНИЕ ПЕРРЕНАТ-АНИОНА НА МИКРОГРАНИЦЕ МЕЖДУ ДВУМЯ НЕСМЕШИВАЮЩИМИСЯ РАСТВОРАМИ ЭЛЕКТРОЛИТОВ

Л.Ю. Мартынов[1,@], Е.В. Лопатухин[1], А.А. Астафьев[2], А.М. Шахов[2], В.А. Надточенко[2], Н.К. Зайцев[1]

[1]МИРЭА – Российский технологический университет (Институт тонких химических технологий имени М.В. Ломоносова), Москва 119571, Россия
[2]Институт химической физики имени Н.Н. Семенова РАН, Москва 119991, Russia
[@]Автор для переписки, e-mail: l.y.martynov@gmail.com

Настоящая работа посвящена изучению простого ионного переноса перренат-иона через поляризуемую микрограницу раздела фаз двух несмешивающихся растворов электролитов (микро-ГРДНРЭ) и применению данного явления для аналитического определения рения. Для создания системы с микро-ГРДНРЭ изготовлена микроперфорированная полимерная мембрана из полиэтилентерефталата , в которой с помощью фемтосекундного лазера проделан массив из 196 микроотверстий диаметром 10±0.1 мкм. С использованием данной системы методом циклической вольтамперометрии (ЦВА) впервые исследованы первичные характеристики переноса перренат-иона на микрогранице раздела фаз вода/2-нитрофенилоктиловый эфир и определены термодинамические параметры переноса, такие, как формальный потенциал ионного переноса, энергия Гиббса и межфазный коэффициент распределения. Для повышения чувствительности обнаружения перренат-иона применяли также технику инверсионной вольтамперометрии (ИВА). При оптимизированных условиях электрохимического концентрирования и обнаружения достигнут предел обнаружения перренат-иона, равный 0.3 мкМ, с широким линейным динамическим диапазоном от 1.0 до 100 мкМ. Изучено влияние х мешающих ионов на электрохимический отклик перренат-иона, и достигнута отличная селективность по отношению к анионам SCN^-, I^-, NO_3^-, NO_2^-, CO_3^{2-}, SO_4^{2-}, MoO_4^{2-}, WO_4^{2-} и CH_3CO^-. Это позволило провести количественное определение рения в некоторых образцах минерального сырья и сравнить полученные данные с результатами, полученными методом атомно-эмиссионной спектроскопии с индуктивно связанной плазмой.

Ключевые слова: *перренат-ион, вода/2-нитрофенилоктиловый эфир, микро-ГРДНРЭ, реакция ионного переноса, фемтосекундный лазер, инверсионная вольтамперометрия.*

1. Introduction

The analysis of various species of rhenium is of great importance due to its unique physicochemical properties and wide application in various fields of chemical, aerospace and nuclear industries [1, 2]. In particular, due to high refractoriness, mechanical strength and chemical inertness, rhenium is a valuable material for the manufacture of steels and alloys for turbines of jet engines, high-temperature thermocouples and components of electronic contacts and electromagnets. In addition, rhenium has proven itself in the production of rhenium-platinum catalysts used in petroleum reforming for the production of high-octane hydrocarbons, which are used in the production of lead-free gasoline [3]. The estimated value of rhenium consumed in 2017, was about $ 80 million [4].

Rhenium is a rare element: its content in the Earth's crust is about 7×10^{-8} % by weight [5]. The most important raw sources of rhenium are sulfide (molybdenum and copper) and carbonaceous (uranium) concentrates. Minerals of rhenium themselves are extremely rare in nature.

There was a requirement of extraction of rhenium from secondary raw materials, industrial waters and plants due to its high cost and small content in natural materials [6]. Both analyzed natural and technogenic rhenium-containing raw materials have a complex and diverse composition. The content of rhenium in rhenium-containing raw materials varies in a wide range of concentrations – from 10^{-7} to tens of weight percent. This leads to the creation and improvement of methods for its analytical control in different materials [7].

In modern analytical practice, methods such as inductively coupled plasma atomic emission spectroscopy (ICP AES) [8], inductively coupled plasma – mass spectrometry (ICP-MS) [9], X-ray fluorescence analysis [10] and spectrophotometric methods [11] are used for direct determination of rhenium in the aqueous phase. Although these methods provide reliable, accurate and reproducible analysis, their sensitivity is not sufficient for direct determination of rhenium due to low element contents in the analyzed objects and the interfering effect of matrix components. Moreover, implementation of these methods requires expensive equipment, as well as collection and transportation of environmental samples for laboratory analysis.

Electrochemical methods take a significant place in the analytical chemistry of rhenium due to the high speed and accuracy of the analysis, the possibility of miniaturization, as well as high sensitivity and selectivity. In particular, direct voltammetric determination of rhenium based on measurement of diffusion waves of the recovery of perrhenate ions and indirect determination using different types of mercury-film and carbon electrodes in conjunction with linear sweep or stripping voltammetry are reported [12–14]. For instance, the adsorptive accumulation of rhenium in the form of a rhenium oxide film of low solubility onto a polyethylene-impregnated graphite electrode followed by the oxidation of the adsorbed species using square-wave voltammetry was developed for Re(VII) ion analysis with a detection limit of 0.8 nM. Nevertheless, the selectivity of the voltammetric analysis of rhenium is rather low due to the interfering effect of metal ions (Mo, W, Cu, Ag, Au ions) occupying a higher position on the scale of standard potentials than the perrhenate ion.

An alternative to solid-electrode-based voltammetry for rhenium analysis is the transfer reaction at a polarized interface between two immiscible electrolyte solutions (ITIES) [15]. The ITIES method is based on reversible ion transfer across a polarized liquid-gel interface upon application of a potential difference. Ion transfer from one phase to another gives rise to a current that can be monitored. On this basis, a sensitive and selective platform is realized for amperometric sensing of various inorganic ions in aqueous solutions, as well as organic compounds that do not decompose into ions [16]. For a long time, the analytical use of the ITIES method with a large liquid interface was mainly due to mechanical instability and uncompensated ohmic losses due to the strong resistivity of the organic phase. The solution to this problem was the approach demonstrated by Campbell and Girault [17] based on the use of the micro-liquid/gel interface supported on a microporous polymeric membrane. The use of microporous polymeric membrane-supported ITIES made it possible to significantly simplify the experimental design of the method and served as the basis for creating new platforms for arrays of micro-interfaces for portable sensors [18–20].

In this paper, the reaction of simple transfer of perrhenate ions at the water/2-nitrophenyloctyl ether (2-NPOE) micro-interface array was investigated. The approach to interface miniaturization used in this study is based on microfabricated porous polyethylene terephthalate (PET) membranes prepared by femtosecond laser-etching processes. The characteristics of perrhenate ion transfer reaction were studied using cyclic voltammetry (CV) and alternating current stripping voltammetry (ACSV). The thermodynamic parameters for the perrhenate ion transfer are discussed. The effect of interfering ions on the obtained analytical perrhenate signal is also estimated. Stripping analysis at the micro-liquid/liquid interface arrays is suitable for the detection of analytes in rhenium containing alloys and mineral raw materials.

2. Experimental

2.1. Reagents

2-Nitrophenyloctyl ester (2-NPOE, Sigma-Aldrich), tetradodecylammonium tetrakis(4-chlorophenyl)borate (TDATpClPB, Fluka), magnesium sulfate ($MgSO_4$, Chimmed Co.), tetramethylammonium chloride (TMACl, Sigma-Aldrich), polyvinylchloride (PVC, high molecular weight, BSK Co.), potassium perrhenate ($KReO_4$, Sigma-Aldrich), sodium hydroxide (NaOH, Sigma-Aldrich), sodium molybdate ($Na_2MoO_4 \cdot 2H_2O$, Acros Organics), sodium tungstate ($Na_2WO_4 \cdot 2H_2O$, Acros Organics), rhenium (Re, Sigma-Aldrich), sulfuric acid (H_2SO_4, Acros Organics), hydrogen peroxide solution (30% H_2O_2, Sigma-Aldrich) were all used as received. All aqueous solutions were prepared using bidistilled water.

2.2. Fabrication of microhole array-liquid/liquid interface

A 196 (14×14) microhole array was created by drilling a polyethylene terephthalate film (PET, 10 μm thick, from Vladipor LTD, Russia) using the previously reported method [17] with a modification: the micromachining of the hole was performed using nonlinear ultrafast laser photoablation processing by a femtosecond Ti:Sapphire laser. Compared with other machining techniques, this method provides an advantage of localized, precise and reproducible material processing [21]. Femtosecond laser pulses at 790 nm were amplified in a four-pass laser amplifier up to 2 μJ energy and coupled to the Olympus IX71 optical microscope. Pulses were focused into a 2 μm focal spot by an objective lens (Newport M-10× 0.25NA). Cylindrical holes were drilled in a film using a programmed circular movement performed by a 2D piezo-stage (NT MDT) with a 100 nm step, at each step the film was processed with a single pulse. The average radius of each microhole was determined as around 10 μm both for the entrance and exit side, while the average centre-to-centre distance between two neighboring microholes in the 196 microhole array (approximately 100 μm) is at least 10 times larger than that of each microhole radii (Fig 1).

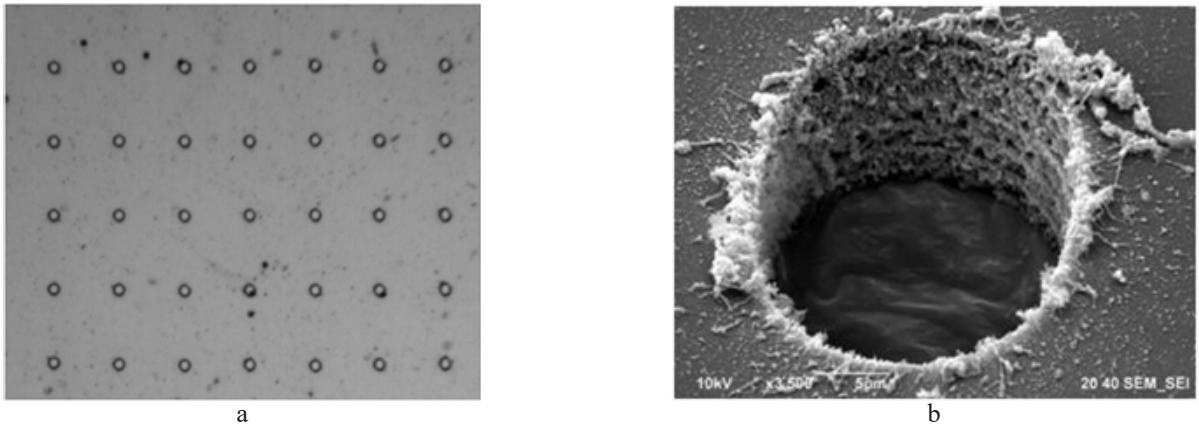

a b

Fig. 1. Scanning electron micrographs of microperforated PET membrane (a) and representative image of 20 μm single microhole (b).

Twenty microliters of the organic solution composed of 5% PVC and 10 mM TDATpClPB dissolved in 2-NPOE were casted onto the laser-machined PET film over the micro-hole array region at a 80 °C and kept for a minimum of 6 h at room temperature to cool down and form a gelified layer.

2.3. Electrochemical measurements

All electrochemical experiments were performed using potentiostat Ecotest-VA-4 (Econix-Expert Ltd., Russia) together with the Ecotest VA software supplied with the instrument. Despite the fact that the IR drop effect at micro-ITIES system is not too high as compared to macro-ITIES system, in this study a four-electrode electrochemical cell was employed. The reference electrode in the aqueous phase was an Ag/AgCl electrode. The reference electrode in the organic phase was an Ag/AgTpClPB electrode made by electrochemical oxidation of a silver wire in a 0.1 M solution of TDATpClPB. Two platinum counter electrodes placed in the aqueous and 2-NPOE phases were used for supplying the current flow (see the schematic presentation in Fig. 2a inset).

The borosilicate glass tube with PET-membrane sealed to one end with silicone sealant contained 200 microliters of the organic solution of 10 mM of TDATpClPB in 2-NPOE. This was then immersed in 25 mL of the aqueous phase 10 mM solution of $MgSO_4$.

All measurements were carried out at room temperature without any IR drop compensation by cyclic voltammetry (CV), alternating current voltammetry (ACV) and alternating current stripping voltammetry (ACSV) technique with a modulation amplitude of 50 mV and a pulse frequency of 5 Hz. The parameters pre-concentration potential, pre-concentration time and sweep rate were explored to determine the optimum values, and these were implemented in subsequent experiments. The scan rate for cyclic voltammetry experiments was 12 mV s^{-1} unless otherwise stated.

3. Results and Discussion

3.1. Electrochemical characterization of perrhenate anion transfer across a micro-water/gel interface

The simple transfer of perrhenate ion across the microhole array interface between water and a PVC-NPOE gel layer incorporating TDATpClPB as an organic supporting electrolyte were first studied using cyclic voltammetry. The TDATpClPB supporting electrolyte not only helps to keep sufficient conductivity of the organic phase, but also offers a wide polarization window to characterize the voltammetric response of perrhenate anions, which could limit the negative end potential. The process of simple ion transfer of perrhenate anion across the micro-ITIES was studied using conventional electrochemical cell setup in Fig. 2a inset and Cell 1.

AgTpClPB/Ag RE	Organic reference electrolyte 10 mM TDATpClPB in NPOE Pt-CE	PET membrane 5% PVC-NPOE 10 mM TDATpClPB	Water 10 mM $MgSO_4$ *x* μM ReO_4^- Pt-CE`	AgCl/Ag RE`	**Cell 1**

where *x* is the concentration of the perrhenate anion in the aqueous phase.

In the absence of perrhenate ion ReO_4^- the potential window was determined by the transfer of the electrolyte ions dissolved in each phase, which resulted in a current rise. At the positive end, the potential window is limited by Mg^{2+} or $TpClPB^-$ ion transfer, while the negative end is set by TDA^+ or SO_4^{2-} ion transfer across the polarized interface [see Fig. 2a]. The clear potential window between –0.40 and +0.60 V is available for studying the ReO_4^- transfer.

The addition of ReO_4^- ions into the aqueous phase resulted in the occurrence of a pseudo-steady state voltammetric response in the cathode region of the potential window on the forward scan, while more pronounced peak-shaped responses were observed on the reverse scan at *ca*. 0.05 V (vs. Ag/AgCl). Such voltammetric characteristics are typically observed when utilizing a microhole-water/PVC-NPOE gel interface with a gel-filled microhole; on the forward scan, ReO_4^- ions transfer from water to the organic gel phase is usually associated with a hemi-spherical diffusion flux that results in a pseudo-steady state current response.

While the peak current for the ion transfer from the organic to the aqueous phase is associated with a hemi-spherical diffusion regime, the reverse flux from the aqueous phase to the hole region is governed by a linear diffusion [22]. This is due to the fact that the incorporation of PVC in the organic phase increases the viscosity, and hence slows down the diffusion of ions in the organogel, so that the diffusion coefficient of a target analyte in the gelled organic phase may be ca. nine times lower than in the aqueous phase [23]. However, in this study, the CVs on the forward scan show that the foot of the ion transfer wave was at a very negative applied potential difference (–0.4 V), close to the upper limit of the potential window (Fig. 2a). The current increased steadily with applied potential up to the switching

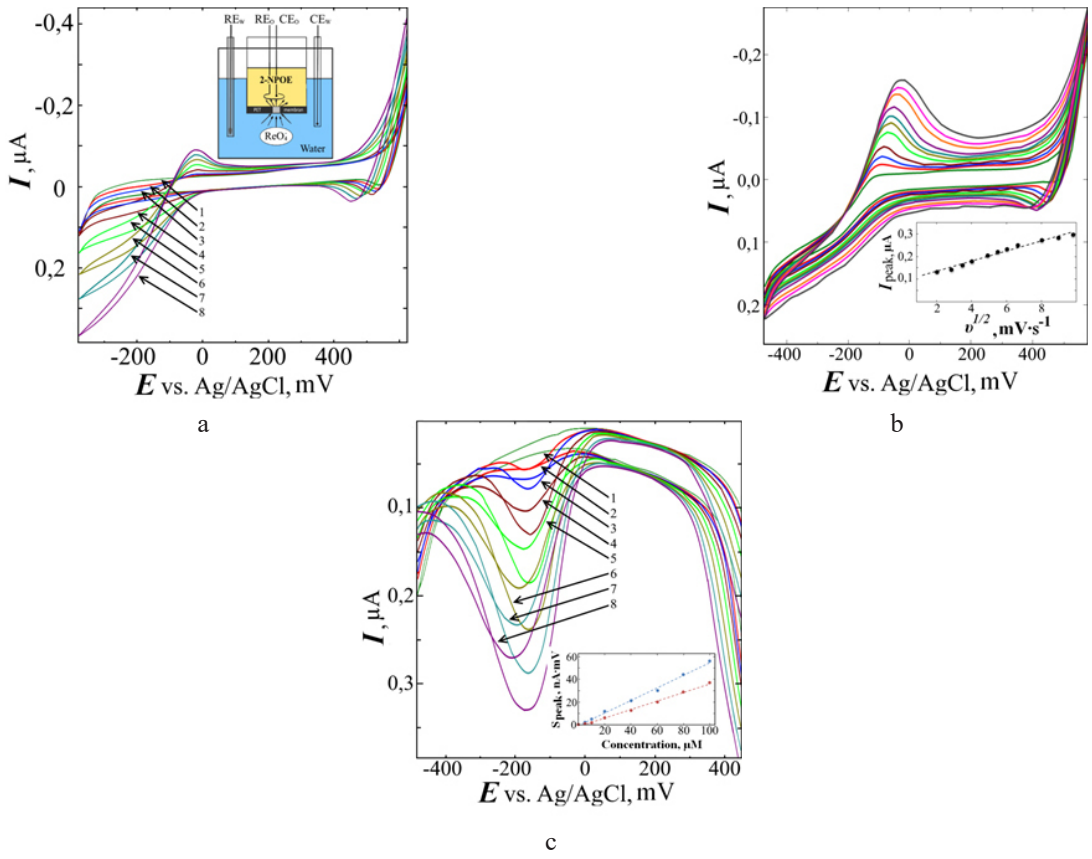

Fig 2. Representative cyclic voltammograms for the simple transfer reaction of different concentrations of ReO_4^- ions across water/NPOE microinterface. Cell 1 was used.
(a) The ReO_4^- ion concentration (x in Cell 1) was varied from 5 to 100 μM. Scan rate was 12 mV s^{-1}. Inset in (a) shows a schematic of the electrochemical system for the study of ion transfer reactions across a micro-liquid/liquid interface.
(b) A series of cyclic voltammograms for the transfer of ReO_4^- ions at different scan rates ranging from 4 to 96 mV s^{-1}. x = 50 in Cell 1 was used. Inset in (b) shows a plot of the peak current versus the square root of the scan rate.
(c) Representative alternating current cyclic voltammograms for different concentrations of ReO_4^- ions transferring across water/NPOE microinterface. Inset in (c) shows a plot of the peak current versus the concentration of perrhenate anion: 1 – 10 mM $MgSO_4$ solution in the absence of ReO_4^-; 2 – 5 μM; 3 – 10 μM; 4 – 20 μM; 5 – 40 μM; 6 – 60 μM; 7 – 80 μM; 8 – 100 μM.

potential, so that a fully-develop steady-state wave shape was not obtained. A similar observation was reported by Osborne and Girault [24] for the transfer of ammonium ions across a water/1,2-dichloroethane (DCE) interface and by Cacote et al. [25] for the direct transfer of Ag^+ ions across a water/DCE interface.

As the concentration of Re(VII) ions increased, the current on both the forward (ReO_4^- ion transfer from water to NPOE) and reverse (from NPOE to water) scans also linearly increased. A linear slope of 2.71 μA mM^{-1} was obtained from a plot of the steady-state current changes (forward) vs. Re(VII) ion concentration, which can be correlated to Saito [26] equation developed for radial diffusion-controlled reversible ion transfer process at an array of microhole-water/gel interfaces:

$$I_{ss}^{FWD} = 4z_i nFD_{ReO_4^-}^{w} C_{ReO_4^-} r \quad (1)$$

where I_{ss}^{FWD} is the steady-state current responsible for the ReO_4^- ion transfer from water to the organic phase, z_i is the charge of the ReO_4^- ion, F is the Faraday constant, $D_{ReO_4^-}^{w}$ is the diffusion coefficient of ReO_4^- ions in the aqueous phase 1.47×10^{-5} cm^2 s^{-1} [27], $C_{ReO_4^-}$ is the concentration of the perrhenate ion in the water phase, and r (10.0 μm) is the radius of the interface. The experimental slope was slightly smaller as compared to the theoretical value of 2.25 μA mM^{-1}.

The peak current response with respect to the scan rate was also investigated (see Fig. 2b), where the peak potential for 50 μM ReO_4^- ion transfer was found to be almost independent of the scan rate. When plotting the current versus the square root of scan rate (see Fig. 2b inset), a linear relationship with a slope of 0.022 μA (V s^{-1})$^{-1/2}$ also obtained. This value

was slightly smaller than 0.033 μA (V s^{-1})$^{-1/2}$, which was obtained from Randles-Sevcik equation developed for a diffusion-controlled reversible ion transfer process across a polarized ITIES:

$$I_P = 0.4463 z_i AFC_{\mathrm{Re}O_4^-} \sqrt{\frac{z_i F}{RT}} \sqrt{\upsilon} \sqrt{D_i} \quad (2)$$

where I_P is the peak current responsible for Re(VII) ion transfer from the organic to the water phase, A is the area of the liquid/liquid interface, R is the gas constant, T is the absolute temperature, and v is the scan rate. The differences in both the linear fit values for the concentration and scan rate dependence can be attributed to possible errors coming from the estimation of the exact liquid/liquid interface size. In addition, the peak to peak separation was about 7.5 mV and changed little with respect to the scan rate change. These results indicate that the ReO_4^- ion transfer reaction is regarded as a reversible diffusion-controlled process.

In order to further enhance sensitivity alternating current voltammetry (ACV) was applied, Fig. 2c. In the absence of the perrhenate ion ReO_4^- the potential window is restricted by the transfer of background electrolyte ions and resembles the shape of a bath. When increasing the scan rate (8–99 mVs^{-1}) and amplitude modulation (5–50 mV), background current increases from 0.02 to 0.40 μA. In this case voltamperograms are not distorted. The addition of different concentrations of the perrhenate ion ReO_4^- (5–100 μM) in aqueous solution induces a broad voltammetric peak on the forward and reverse scans at ca. –0.16 V (vs. Ag/AgCl). The separation of the peaks increased with respect to the ReO_4^- ion concentration ranging from 5 to 100 μM and was about 42.5 mV at the concentration of the perrhenate ion 100 μM. A peak current area increased proportionally as a function of the perrhenate ion ReO_4^- concentration. A notable fact is that ACV response of the ReO_4^- ion has a greater intensity of current in absolute value. This result is very interesting for increasing the sensitivity of the sensor for the perrhenate ion in a very simple way (changing only the modulation amplitude or scan rate). The resulting ACV peaks area current was also plotted against various concentrations of target ions (Fig. 2c inset). As can be seen, from the plot of the ACV peak area current versus the ReO_4^- concentration a linear fit with a slope of 57.6 μA mV mM^{-1} for the Re(VII) concentration ranging from 5 to 100 μM was obtained.

3.2. Thermodynamic parameters of ReO_4^- transfer at the water/NPOE interface

A number of thermodynamic parameters for the ReO_4^- ion transfer were determined from the CV data. These are listed in Table 1.

Table 1. Thermodynamic data for the transfer of ReO_4^- ion at the micro-water/NPOE interface arrays

Parameter	$\Delta_o^w\varphi^0_{\mathrm{Re}O_4^-}$	$\Delta_o^w\varphi^0_{\frac{1}{2},\mathrm{Re}O_4^-}$	$\Delta_O^W G^0_{tr,i}$	$\lg P_{2-NPOE}(ReO_4^-)$	$D^w_{\mathrm{Re}O_4^-}$
Value	–0.184 V	–0.264 V	17.8 kJ mol^{-1}	–3.12	14.6×10^{-5}[a] cm^2 c^{-1}

[a]Data obtained from Ref. [26].

The value of the formal transfer potential of an ReO_4^- ion is obtained by transposing the measured experimental value to the Galvani potential scale, as given by the following expression [28]:

$$\Delta_o^w\varphi^0_{\mathrm{Re}O_4^-} = \Delta_o^w\varphi_{\mathrm{Re}O_4^-} - \Delta_o^w\varphi_{TMA^+} + \Delta_o^w\varphi^0_{TMA^+} \quad (3)$$

where $\Delta_o{}^w\varphi_{(TMA+)}{}^0$ is the formal transfer potential of the TMA^+ ion, $\Delta_o{}^w\varphi_{(ReO4-)}$ and $\Delta_o{}^w\varphi_{(TMA+)}$ are the experimental potentials of the ReO_4^- ion and TMA^+ ion, respectively.

In this study, a value of +0.140 V was used for $\Delta_o{}^w\varphi_{(TMA+)}{}^0$ [29]. TMA^+ ion was selected as a model ion, since the transfer potential differs from that of ReO_4^- ion, and there is no mutual interference. The calculated Galvani transfer potential of ReO_4^- ion across a water/NPOE interface is obtained using Eq. (3) to be –0.184 V (Table 1).

A value for the half-wave transfer potential of the ReO_4^- ion can be obtained using Eq (4):

$$\Delta_o^w\varphi^0_{\frac{1}{2},\mathrm{Re}O_4^-} = \Delta_o^w\varphi_{\frac{1}{2},\mathrm{Re}O_4^-} - \Delta_o^w\varphi_{\frac{1}{2},TMA^+} + \Delta_o^w\varphi^0_{TMA^+} \quad (4)$$

where $\Delta_o^w\varphi_{\frac{1}{2},\mathrm{Re}O_4^-}$ and $\Delta_o^w\varphi_{\frac{1}{2},TMA^+}$ are the experimental half-wave potentials of the ReO_4^- ion and TMA^+ transfer, respectively. The $\Delta_o^w\varphi^0_{\frac{1}{2},\mathrm{Re}O_4^-}$ of the ReO_4^- ion is obtained using Eq. (4) to be 0.264 V (Table 1).

The Gibbs energy of transfer is directly related to the formal transfer potential of the ion transfer [30] and for any ionic species is expressed as:

$$\Delta_O^W\varphi_i^0 = \frac{\Delta_O^W G^0_{tr,i}}{z_i F} \quad (5)$$

where $\Delta_o{}^w\,G_{(tr,i)}{}^0$ is the formal Gibbs transfer energy of the ion from the aqueous (w) to the organic (o) phase. The ability to measure this value depends on the

condition that the transferring ion has a lower magnitude of the Gibbs transfer energy than the ions of the supporting electrolytes. The calculated value is presented in Table 1. The formal Gibbs energy of transfer of the ReO_4^- ion was 17.8 kJ mol^{-1} across a water/NPOE interface. Values of 16.9 and 20.1 kJ mol^{-1} have been reported previously for the perchlorate ion (ClO_4^-) transfer across a water/NPOE interface [29] and the permanganate ion (MnO_4^-) transfer across a water/*o*-dichlorobenzene interface [31], respectively. This suggests that that the perrhenate anion has a similar hydrophobicity and occupies an intermediate position in the general scale of standard ion transport energies in systems with different organic solvents.

Another important thermodynamic parameter is the coefficient (lgP_{NPOE}) of a given solute partition between two immiscible solvents. This is a measure of its relative affinity for the two phases, and is related to the free energy of transfer of the solute between the two solvents. The coefficient of the perrhenate ion ReO_4^- partition between water and 2-NPOE is obtained from Eq. (6) [32]:

$$\lg P_{2-NPOE}(\mathrm{Re}O_4^-) = -\frac{\Delta_O^W G_{tr,i}^0}{2.3RT} \quad (6)$$

The partition coefficient of the perrhenate ion was –3.12 (Table 1), while the value for the perchlorate ion was –2.96 [33], both for the water/2-NPOE system. Comparison of the partition coefficients of both ions shows that perrhenate is more hydrophobic, since a higher partition coefficient value indicates a more hydrophobic property. A review of the electrochemical investigations made on the transfer of ions and ionic species at ITIES to determine their partition coefficients employing voltammetric methods for water/nitrobenzene (NB), water/2-NPOE, and water/DCE systems does not include any data for the perrhenate ion.

3.3. Optimisation of the ACSV parameters for the detection of ReO_4^- ions

In order to detect lower concentrations, ACSV was employed, as this entails a pre-concentration step that enhances sensitivity. In the pre-concentration step, the ReO_4^- ions were extracted from the aqueous to the organogel phase under potential control. Then, the pre-concentrated analyte was stripped out of the organogel using a voltammetric scan. The pre-concentration step is important in ACSV as it enables the detection of lower concentrations relative to CV. As a result, the optimization of ACSV parameters, namely the sweep rate, the pre-concentration potential and the pre-concentration time were explored employing Cell 1. Voltammetric scans were conducted in the positive direction, from –0.5 to 0.6 V.

To assess the impact of sweep rate on the results (figure not shown), the sweep rate value was varied between 5 and 100 mV s^{-1} using 5×10^{-6} M ReO_4^- ion. The pre-concentration potential was fixed at –0.40 V, while the pre-concentration time was set at 60 s. A blank ACSV was recorded in the absence of the analyte, so that background-subtracted ACSV could be obtained by subtracting the blank response from that of the analyte. The stripping peak current was found to be linearly-dependent on the square root of the sweep rate, indicating a linear diffusion-controlled organic phase to aqueous phase transfer process [34]. Despite this result, it was found that lower sweep rates produced a more clearly defined peak shape consistent with peak distortion by cell resistance and capacitance at the higher sweep rates. Consequently, all subsequent experiments employed a sweep rate of 12 mV s^{-1}, since this sweep rate produced a well-defined peak shape with less sensitivity to these distortions.

The influence of the pre-concentration potential was studied by employing 5.0 μM ReO_4^- with a 60 s pre-concentration time, while varying the pre-concentration potential from –0.40 to 0.20 V in increment of 0.05 V, Fig. 3a. From the inset graph, it can be seen that the stripping peak current decreases when the pre-concentration potential shifts to the positive area. As observed earlier by CV, ReO_4^- transfers at an applied potential very close to the upper limit of the potential window. The maximum stripping peak current was observed when the pre-concentration potential was –0.40 V. Thus, this potential was applied for all subsequent experiments.

The influence of pre-concentration time was studied at –0.40 V pre-concentration potential using 5 μM ReO_4^-, with variations in the pre-concentration time from 30 to 360 s (Fig. 3b). The stripping peak current increased as the pre-concentration time increased, eventually reaching a constant value, as illustrated in the inset graph. This effect was reported previously for the detection of perchlorate [35] and hexachromic anions [36] at the micro-ITIES array and was attributed to the diffusion of the analyte away from the interface to the bulk organic phase during the longer pre-concentration times. Therefore, during the stripping step, these analytes are not stripped back to the aqueous phase and do not contribute to the stripping peak. The optimum pre-concentration time of 90 s was selected and applied in all subsequent experiments.

Employing all of the optimized parameters (12 mV s^{-1} sweep rate, –0.40 V pre-concentration potential, 90 s pre-concentration time), low concentrations of ReO_4^- in the range 1.0–100.0 μM were analysed, and a calibration graph of stripping peak current versus concentration of ReO_4^- ion was plotted (Fig. 4).

The stripping peak increased linearly with respect to the ReO_4^- ion concentration (Fig. 4 inset) with a linear concentration dependence observed within the range studied. An excellent detection limit of 0.3 μM using

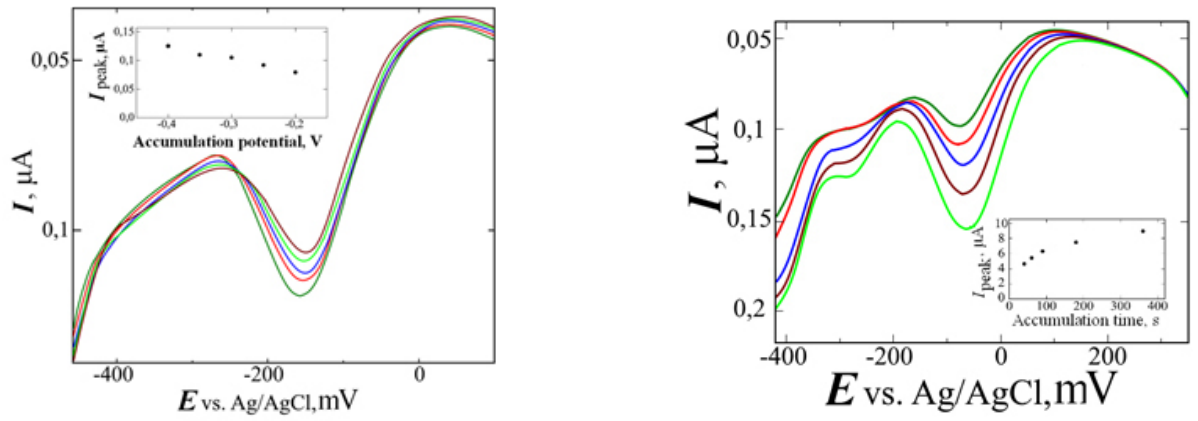

a b

Fig. 3. Influence of pre-concentration potentials from –0.4 V (dark green) to –0.2V (black) in increment of 0.05V on the ACSV of 5 μM ReO_4^- ion (a). The pre-concentration time and sweep rate were fixed at 60 s and 12 mV s^{-1}, respectively. Inset: graph of current at selected pre-concentration potentials of –0.40, –0.35, –0.30, –0.25 and –0.20 V. Influence of pre-concentration times on the ACSV of 5 μM ReO_4^- ion (b). The pre-concentration potential and sweep rate were fixed at –0.40 V and 12 mV s^{-1}, respectively. ACSV response of 30 (dark green), 60, 90, 180 and 360s (light green) pre-concentration times. Inset: calibration graph of peak current versus pre-concentration times.

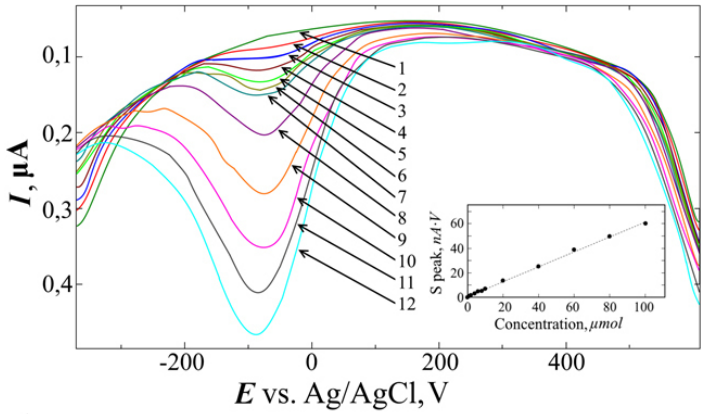

Fig. 4. Representative alternating current stripping voltammograms (ACSV) for the sensing of perrhenate anions at the micro-ITIES arrays. The voltammogram was scanned from low to high potentials to strip the preconcentrated perrhenate ion from the organic gel layer to the aqueous phase. A 90 s of pre-concentration by means of holding the potential of –400 mV was used to accumulate ReO_4^- anions in the gel layer before the stripping. Cell 1 was used where *x* was varied from 1 to 100. Inset shows the calibration curve of ACSV peak area current versus the concentration of ReO_4^- anions: 1 – 10 mM $MgSO_4$ solution in the absence of ReO_4^-; 2 – 1 μM; 3 – 2 μM; 4 – 4 μM; 5 – 6 μM; 6 – 8 μM; 7 –10 μM; 8 – 20 μM; 9 – 40 μM; 10 – 60 μM; 11 – 80 μM; 12 – 100 μM.

a signal to noise ratio of 3:1 was established, which comfortably exceeds the requirements for detecting the perrhenate ion in environmental samples. The LOD obtained for the perrhenate anion is of the same order of magnitude of those found by other investigators by stripping voltammetry.

3.4. Amperometric ReO_4^- ion selective sensors for real sample analysis

The selectivity of the sensor for ReO_4^- ions was finally investigated in the presence of different interfering anionic species (*y* or *z* in Cell 2) including SCN^-, I^-, NO_3^-, NO_2^-, CO_3^{2-}, SO_4^{2-}, MoO_4^{2-}, WO_4^{2-}, and CH_3COO^- anions was investigated at a fixed concentration of 10 μM perrhenate ions. Cell 2 was used.

AgTpClPB/Ag RE	10 mM TDATpClPB in NPOE Organic reference electrolyte Pt-CE	PET membrane 5% PVC-NPOE 10 mM TDATpClPB	Water 10 μmol dm^{-3} ReO_4 1 mmol dm^{-3} Na*y* or Na_2z Pt-CE`	AgCl/Ag RE`	**Cell 2**

These ions were selected, since they are all models of substances likely to be present in ore concentrates and natural water samples. The interfering ions were investigated at a fixed concentration of 1 mM, which is a hundred times in excess compared to that of ReO_4^- ions. The selectivity coefficient (log $k_{(i,j)}^{amp}$) for all the interfering anions studied are listed in Table 2 calculated using the Eq (7) [37]:

$$k_{i,j}^{amp} = (I_t - I_i) C_i / I_i C_j \quad (7),$$

where i and j correspond to the ReO_4^- and interfering ions, respectively, C is the concentration of each ion species, and I_t is the total current, which is the sum of the current associated with the ReO_4^- ion (I_i) and other interfering ions.

Table 2. Summary showing amperometric selectivity coefficients of ReO_4^- ion detection responses over different interfering ions

Interfering ion	SCN^-	NO_3^-	NO_2^-	CO_3^{2-}	SO_4^{2-}	MoO_4^{2-}	WO_4^{2-}	CH_3COO^-
$\lg k_{i,j}^{amp}$	–0.585	–2.564	–1.982	n.i.	n.i.	n.i.	n.i.	n.i.

n.i. – not interfering

In the hundred times excess presence of CO_3^{2-}, SO_4^{2-}, CH_3COO^- anions, the ReO_4^- sensor did not show any responses. The hundred times excess of MoO_4^{2-} and WO_4^{2-} ions, which are usually present in the ore together with rhenium, does not affect the response of the sensor. However, for the hundred times excess of SCN^-, NO_2^- and NO_3^- anions, the perrhenate sensor responded significantly. Nevertheless, the simultaneous presence of these ions together with perrhenate in real objects is unlikely.

3.5. Determination of ReO_4^- ion in mineral raw

As a final demonstration, the sensor was applied to the detection of rhenium in mineral raw samples. The first sample was rhenium itself, and the other two different samples were prepared by adding different amounts of potassium perrhenate to the dolomite and copper-zinc pyrite ore. For dissolution the analyzed sample was treated with a mixture of conc. H_2SO_4 and H_2O_2 (36%) taken in a 3:1 ratio, and then the resulting solution was neutralized with 1M NaOH. Details of the sample preparation are described in [12].

The determination of perrhenate in mineral raw as the aqueous phase electrolyte solution was conducted using Cell 3.

The ACSV analysis data using our perrhenate sensor were also compared to those of the standard ICP-AES analysis method summarized in Table 3.

AgTpClPB/Ag RE	Organic reference electrolyte 10 mM TDATpClPB in NPOE Pt-CE	PET membrane 5% PVC-NPOE 10 mM TDATpClPB	Real sample *x* μmol dm^{-3} $KReO_4$ Pt-CE	AgCl/Ag RE`	**Cell 3**

Table 3. Comparison of real sample analyses utilizing the microhole array-water/NPOE sensor and ICP-AES method

Sample number[a]	Added perrhenate ion concentration (μM)	Our method verification (Conc. (μM) in undiluted sample ± error)	ICP-AES method (Conc., μM)	S_r
1	10	11 ± 3	10	0.15
2	50	56 ± 7	55	0.12
3	100	106 ± 11	110	0.11

[a]Sample 1 is the sample of metallic rhenium; Samples 2 and 3 are the dolomite and copper-zinc pyrite ore spiked with the perrhenate concentration of 50 and 100 mM respectively.

It was found that the added concentrations of ReO_4^- estimated using our sensors in ore samples were in good agreement with the data within a S_r 15% error. An excellent agreement achieved in both the portable sensing and conventional ICP-AES method indicates that our method can be utilized for real-time analysis of perrhenate anions in any environmental mineral raw samples.

4. Conclusions

Voltammetric responses of simple transfer of ReO_4^- ions across the microhole array-water/organic gel interface was investigated. The results show that ReO_4^- ions can be detected via CV and ASV. Important characteristics of ReO_4^- ion transfer across the micro-ITIES – the reversibility, formal transfer potential, the

Gibbs energy of transfer and the partition coefficient – were evaluated and then usefully employed. In addition, employing the ACSV, the detectable concentration of ReO_4^- ions down to 0.3 μM was obtained with a dynamic range of 1 to 100 μM. The novel amperometric ReO_4^- ion selective sensor was successfully applied to determine the perrhenate anion concentration in mineral raw samples, and the results were in good agreement with the data from a conventional ICP-AES method. The results point to the development of a useful sensor based on micro-ITIES that can be used for the detection of the perrhenate ion in environmental systems.

Acknowledgement

This research was supported by Russian Science Foundation grant No 17-73-10430.

References:

1. Emsley J. Rhenium. Nature's Building Blocks: An A–Z Guide to the Elements. Oxford University Press, England, UK, 2001. 699 p.

2. Palant A.A., Troshkina I.D., Chekmarev A.M. Metallurgy of Rhenium. Moscow: Nauka Publ., 2007. 298 p. (in Russ.).

3. Pritchard J., Ciftci A., Verhoeven E., Hensen J.M., Pidko E.A. Supported Pt-Re catalysts for the selective hydrogenation of methyl and ethyl esters to alcohols. *Catal. Today.* 2017; 279(1): 10-18.

4. Polyak D.E. U.S. Geological Survey, Mineral Commodity Summaries, Rhenium [Electronic resource] – https://minerals.usgs.gov/minerals/pubs/commodity/rhenium/index.html (accessed on 03/14/2018).

5. Greenwood N.N., Earnshaw A. Chemistry of the Elements. Moscow: BINOM Publ., 2015. 1277 p. (in Russ.).

6. Borisova L.V., Ryabukhin V.A., Bozhkov O.D., Tsvetkova Kh.Ts. Field determination of rhenium in plants using catalytic test methods with dimethyldithiooxamide and Sulfonitrazo P. *J. Anal. Chem.* 2010; 65(5): 535-541.

7. Evdokimova O.V., Pechishcheva N.V., Shunyaev K.Yu. UptoDate methods for the determination of rhenium. *J. Anal. Chem.* 2012; 67(9): 741-753.

8. Karadjov M., Velitchkova N., Veleva O., Velichkov S., Markov P., Daskalova N. Spectral interferences in the determination of rhenium in molybdenum and copper concentrates by inductively coupled plasma optical emission spectrometry (ICP-OES). *Spectrochim. Acta B.* 2016; 119(1): 76-82.

9. Li J., Zhong L., Tu X., Liang X., Xu J. Determination of rhenium content in molybdenite by ICP–MS after separation of the major matrix by solvent extraction with N-benzoyl-N-phenylhydroxalamine. *Talanta.* 2010; 81(1): 954-958.

10. Kolpakova N.A., Buinovsky A.S., Mel'nikova I.A. Determination of rhenium in gold-containing ores by X-ray fluorescence spectrometry. *J. Anal. Chem.* 2009; 64(2): 144-148.

11. Lenell B.A., Arai Y. Evaluation of perrhenate spectrophotometric methods in bicarbonate and nitrate media. *Talanta.* 2016; 150(1): 690-698.

12. Goltz L.G., Kolpakova N.A. Sorbtion concentration and determination of the perrenate ions by the stripping voltammetry in mineral raw materials. *Izvestija Tomskogo politehnicheskogo universiteta* (Proceedings of the Tomsk Polytechnic University). 2006; 309(6): 77-80. (in Russ.).

13. Kolpakova N.A., Goltz L.Z. Determination of rhenium in mineral raw materials by stripping voltammetry. *J. Anal. Chem.* 2007; 62(3): 377-381.

14. Oskina Y.A., Gorchakov E.V., Kolpakova N.A. Determination of rhenium by a voltammetric method. *Fundamental'nye issledovanija* (Fundamental Studies). 2013; 8: 687-691. (in Russ.).

15. Samec Z., Samcová E., Girault H.H. Ion amperometry at the interface between two immiscible electrolyte solutions in view of realizing the amperometric ion-selective electrode. *Talanta.* 2004; 63(1): 21-32.

16. Vallejo L.J., Ovejero J.M., Fernandez R.A., Dassie S.A. Simple ion transfer at liquid/liquid interfaces. *Int. J. Electrochem.* 2012; 2012: 1-34.

17. Campbell J.A., Girault H.H. Steady state current for ion transfer reactions at a micro liquid /liquid interface. *J. Electroanal. Chem.* 1989; 266(4): 465-469.

18. Herzog G., Beni V. Stripping voltammetry at micro-interface arrays: A review. *Anal. Chimica Acta.* 2013; 769(1): P. 10-21.

19. Liu S., Li Q., Shao Y. Electrochemistry at micro- and nanoscopic liquid/liquid interfaces. *Chem. Soc. Rev.* 2011; 40(5): 2236-2253.

20. Lee H.J., Beattie P.D., Seddon B.J., Osborne M.D., Girault H.H. Amperometric ion sensors based on laser-patterned composite polymer membranes. *J. Electroanal. Chem*. 1997; 440(1-2): 73-82.

21. Gattass R.R., Mazur E. Femtosecond laser micromachining in transparent materials. *Nature Photonics.* 2008; 2: 219-225. http://dx.doi.org/10.1038/nphoton.2008.47

22. Josserand J., Morandini J., Lee H.J., Ferrigno R., Girault H.H. Finite element simulation of ion transfer reactions at a single micro-liquid liquid interface supported on a thin polymer film. *J. Electroanal. Chem.* 1999; 468(1): 42-52.

23. Strutwolf J., Scanlon M.D., Arrigan D.W.M. Electrochemical ion transfer across liquid/liquid interfaces confined within solid-state micropore arrays – simulations and experiments. *Analyst.* 2009; 134(1): 148-158.

24. Osborne M.D., Girault H.H. Amperometric detection of the ammonium ion by facilitated ion transfer across the interface between two immiscible electrolyte

solutions. *Electroanalysis.* 1995; 7(5): 425-434.

25. Cacote M.H.M., Pereira C.M., Tomaszewski L., Girault H.H., Silva F. Ag^+-transfer across the water/1,2-dichloroethane interface facilitated by complex formation with tetraphenylborate derivatives. *Electrochim. Acta.* 2004; 49(2): 263-270.

26. Saito Y. A theoretical study on the diffusion current at the stationary electrodes of circular and narrow band types. *Rev. Polarogr.* 1968; 15(1): 177-187.

27. Rulfs C.L., Elving P.J. Oxidation levels of rhenium. I. Polarographic and coulometric reduction of perrhenate. *J. Am. Chem. Soc.* 1951; 73(7): 3284-3286.

28. Reymond F., Chopineaux-Courtois V., Steyaert G., Bouchard G., Carrupt P.A., Testa B., Girault H.H. Ionic partition diagrams of ionisable drugs: pH-lipophilicity profiles, transfer mechanisms and charge effects on salvation. *J. Electroanal. Chem.* 1999; 462(2): 235-250.

29. Wilke S., Zerihun T. Standard Gibbs energies of ion transfer across the water/2-nitrophenyl octyl ether interface. *J. Electroanal. Chem.* 2001; 515(1-2): 52-60.

30. Lam H.T., Pereira C.M., Roussel C., Carrupt P.A., Girault H.H. Immobilized pH gradient gel cell to study the pH dependence of drug lipophilicity. *Anal. Chem.* 2006; 78(5): 1503-1508.

31. Hundhammer B., Mueller C., Solomon T., Alemu H., Hassen H. Ion transfer across the water–*o*-dichlorobenzene interface. *J. Electroanal. Chem.* 1991; 319(1-2): 125-135.

32. Ribeiro J.A., Silva F., Pereira C.M. Electrochemical study of the anticancer drug daunorubicin at a water/oil interface: Drug lipophilicity and quantification. *Anal. Chem*. 2013; 85(3): 1582-1590.

33. Abraham M.H., Acree W.E. Jr., Liu X. Partition of neutral molecules and ions from water to o-nitrophenyl octyl ether and of neutral molecules from the gas phase to *o*-nitrophenyl octyl ether. *J. Solution Chem.* 2018; 47(2): 293-307.

34. Zazpe R., Hibert C., O'Brien J., Lanyon Y.H., Arrigan D.W.M. Ion-transfer voltammetry at silicon membrane-based arrays of micro-liquid–liquid interfaces. *Lab Chip.* 2007; 7(12): 1732-1737.

35. Martynov L.Yu., Mel'nikov A.P., Astaf'ev A.A., Zaitsev N.K. Voltammetric determination of perchlorate ion at a liquid–liquid microscopic interface. *J. Anal. Chem.* 2017; 72(9): 992-998.

36. Hossain Md.M., Lee S.H., Girault H.H., Devaud V., Lee H.J. Voltammetric studies of hexachromic anion transfer reactions across micro water/polyvinylchloride–2-nitrophenyloctylether gel interfaces for sensing applications. *Electrochim. Acta.* 2012; 82(1): 12-18.

37. Macca C., Wang J. Experimental procedures for the determination of amperometric selectivity coefficients. *Anal. Chim. Acta.* 1995; 303(2-3): 265-274.

About the authors:

Leonid Yu. Martynov, Postgraduate Student, I.P. Alimarin Chair of Analytical Chemistry, M.V. Lomonosov Institute of Fine Chemical Technologies, MIREA – Russian Technological University (86, Vernadskogo Pr., Moscow 119571, Russia). E-mail: martynov_leonid@mail.ru.

Evgeniy V. Lopatukhin, Student, I.P. Alimarin Chair of Analytical Chemistry, M.V. Lomonosov Institute of Fine Chemical Technologies, MIREA – Russian Technological University (86, Vernadskogo Pr., Moscow 119571, Russia). E-mail: lopatukhinevgenij@yandex.ru.

Artem A. Astafyev, Ph.D. (Phys. and Math.), Senior Researcher, Laboratory of Bio- and Nanophotonics, Semenov Institute of Chemical Physics of Russian Academy of Sciences (4, Bld. 1, Kosygina St., Moscow19991, Russia). E-mail: astafiev.artyom@gmail.com.

Aleksandr M. Shakhov, Ph.D. (Phys. and Math.), Junior Researcher, Laboratory of Bio- and Nanophotonics, Semenov Institute of Chemical Physics of Russian Academy of Sciences (4, Bld. 1, Kosygina St., Moscow19991, Russia). E-mail: physics2007@yandex.ru.

Viktor A. Nadtochenko, D.Sc. (Chem.), Director of Semenov Institute of Chemical Physics of Russian Academy of Sciences (4, Bld. 1, Kosygina St., Moscow 19991, Russia). E-mail: nadto@icp.ac.ru. ORCID: https://orcid.org/0000-0002-6645-692X.

Nikolai K. Zaitsev, D.Sc. (Chem.), Head of the Chair of Energy Technologies, Systems and Installations, M.V. Lomonosov Institute of Fine Chemical Technologies, MIREA – Russian Technological University (86, Vernadskogo Pr., Moscow 119571, Russia). E-mail: nk_zaytsev@mail.ru.

Об авторах:

Мартынов Леонид Юрьевич, аспирант кафедры аналитической химии им. И.П. Алимарина Института тонких химических технологий им. М.В. Ломоносова ФГБОУ ВО «МИРЭА – Российский технологический университет» (119571, Россия, Москва, пр-т Вернадского, д. 86). E-mail: martynov_leonid@mail.ru.

Лопатухин Евгений Владимирович, студент кафедры аналитической химии им. И.П. Алимарина Института тонких химических технологий им. М.В. Ломоносова ФГБОУ ВО «МИРЭА – Российский технологический университет» (119571, Россия, Москва, пр-т Вернадского, д. 86). E-mail: lopatukhinevgenij@yandex.ru.

Астафьев Артем Александрович, кандидат физико-математических наук, научный сотрудник лаборатории био- и нанофотоники Института химической физики им. Н.Н. Семенова РАН (119991, Россия, Москва, ул. Косыгина, д. 4). E-mail: astafiev.artyom@gmail.com.

Шахов Александр Михайлович, кандидат физико-математических наук, младший научный сотрудник лаборатории био- и нанофотоники Института химической физики им. Н.Н. Семенова РАН (119991, Россия, Москва, ул. Косыгина, д. 4). E-mail: physics2007@yandex.ru.

Надточенко Виктор Андреевич, доктор химических наук, директор Института химической физики им. Н.Н. Семенова РАН (119991, Россия, Москва, ул. Косыгина, д. 4). E-mail: nadto@icp.ac.ru. ORCID: https://orcid.org/0000-0002-6645-692X.

Зайцев Николай Конкордиевич, доктор химических наука, заведующий кафедрой энергетических технологий, систем и установок Института тонких химических технологий им. М.В. Ломоносова ФГБОУ ВО «МИРЭА – Российский технологический университет» (119571, Россия, Москва, пр-т Вернадского, д. 86). E-mail: nk_zaytsev@mail.ru.

For citation: Martynov L.Yu., Lopatukhin E.V., Astafyev A.A., Shakhov A.M., Nadtochenko V.A., Zaitsev N.K. Amperometric determination of perrhenate anion using a microscopic interfaces between two immiscible electrolyte solutions. *Tonkie khimicheskie tekhnologii* / *Fine Chemical Technologies.* 2018; 13(4): 5–16.

Для цитирования: Martynov L.Yu., Lopatukhin E.V., Astafyev A.A., Shakhov A.M., Nadtochenko V.A., Zaitsev N.K. Amperometric determination of perrhenate anion using a microscopic interfaces between two immiscible electrolyte solutions // Тонкие химические технологии / Fine Chemical Technologies. 2018. Т. 13. № 4. С. 5-16.